Treatment efficacy of laser photothermal therapy using gold nanorods

Navid Manuchehrabadi

Department of Mechanical Engineering,
University of Maryland Baltimore County,
1000 Hilltop Circle,
Baltimore, MD 21250, USA
Email: manuch1@umbc.edu

Raheleh Toughiri and Charles Bieberich

Department of Biology,
University of Maryland Baltimore County,
1000 Hilltop Circle,
Baltimore, MD 21250, USA
Email: toughir1@umbc.edu
Email: bieberic@umbc.edu

Hong Cai

Department of Physics,
University of Maryland Baltimore County,
1000 Hilltop Circle,
Baltimore, MD 21250, USA
Email: caihong1@umbc.edu

Anilchandra Attaluri

Department of Mechanical Engineering,
University of Maryland Baltimore County,
1000 Hilltop Circle,
Baltimore, MD 21250, USA
Email: aattalu1@jhmi.edu

Raymond Edziah, Elaine Lalanne and Anthony M. Johnson

Center for Advanced Studies in Photonics Research,
University of Maryland Baltimore County,
1000 Hilltop Circle,
Baltimore, MD 21250, USA
and

Department of Physics,
University of Maryland Baltimore County,
1000 Hilltop Circle,
Baltimore, MD 21250, USA
Email: redziah@umbc.edu
Email: elalanne@umbc.edu
Email: amj@umbc.edu

Ronghui Ma and Liang Zhu*

Department of Mechanical Engineering,
University of Maryland Baltimore County,
1000 Hilltop Circle,
Baltimore, MD 21250, USA
Email: roma@umbc.edu
Email: zliang@umbc.edu
*Corresponding author

Abstract: *In vivo* experiments are performed to induce temperature elevations in implanted prostatic tumours in mice using 0.1 ml commercially available gold nanorod solution injected into the tumour. Tumour shrinkage studies and histological analyses of tumour cell death are conducted, and the equivalent minutes at 43°C (EM_{43}) for inducing tissue thermal damage are estimated based on temperature elevations during the treatment. It has been shown that the laser heating of 15 minutes in the tumour tissue containing gold nanorods is effective to cause irreversible thermal damage to the tumours, with a low laser irradiance on the tumour surface (1.6 W/cm^2). The effectiveness of the heating protocol is demonstrated by tumour shrinkage to 7% of its original volume on the 25th day after the laser treatment and tumour necrosis events observed by histological analyses. The results are consistent with the EM_{43} distribution estimated by possible temperature elevations during the treatment.

Keywords: bioheat transfer; gold nanorods; laser photothermal therapy; histological analysis; tumour shrinkage; EM_{43}.

Biographical notes: Navid Manuchehrabadi is a PhD student at the Department of Mechanical Engineering in the University of Maryland Baltimore County. He received his BS in Biomedical Engineering from University of Science and Research Azad in Tehran, Iran in 2004 and MS degree of Biomedical Engineering from Leibniz University in Hannover, Germany in 2009. His research is mainly focused on experimental and theoretical investigation of laser photothermal therapy for prostate cancer treatment using gold nanorods.

Raheleh Toughiri is a Post-doctoral scientist at Eli Lilly and Company. She received her BS from University of Hamedan (2004), MS and PhD (2013) from University of Maryland Baltimore County. Her research focus was to identify novel substrates of Aurora-A kinase in prostate cancer cells. She discovered

novel and known Aurora-A substrates in different human prostate cancer cell lines. Also she identified novel Aurora-A phosphorylation sites for development of potential therapeutic peptides.

Charles Bieberich is a Professor of Biology in the University of Maryland Baltimore County. He received his BA in Biology from University of Tampa in 1982 and his PhD in Genetics from Johns Hopkins University in 1987. His research at UMBC is focused on fundamental molecular processes of cancer formation and development.

Hong Cai is currently a PhD degree candidate with the Physics Department, University of Maryland Baltimore County. She received her BS degree in Applied Optics in 2005 and MS degree in Optics in 2008 from Nankai University, Tianjin, China. Her ongoing research with Dr. Anthony M. Johnson focuses on the carrier dynamics and nonlinearity in quantum cascade laser and quantum well structures. She is a student member of the Optical Society of America (OSA), American Physical Society (APS) and International Society of Optical Engineering (SPIE).

Anilchandra Attaluri is a Postdoctoral Fellow at the Department of Radiation Oncology & Molecular Radiation Sciences in Johns Hopkins University School of Medicine. He received his BTech from the Jawaharlal Nehru Technological University, India, in 2005 and PhD in Mechanical Engineering from University of Maryland Baltimore County, in 2012. His research is focused on bio-transport, artificial organs, imaging, magnetic nanoparticles and hyperthermia applications in cancer.

Raymond Edziah is a Visiting Assistant Professor at the Department of Physics and Engineering in the Delaware State University. He received his BS (1994) and MS (1999) in Physics from University of Cape Coast, Cape Coast, Ghana and PhD in Physics (2010) from University of Maryland Baltimore County. His research focuses on nonlinear optical characterisation of bulk and nanostructure materials for optical limiting and switching applications.

Elaine Lalanne is an Assistant Research Scientist in the Center for Advanced Studies in Photonics Research at University of Maryland Baltimore County. She received BA in physics from Wellesley College in 1994 and a PhD in Applied Physics from New Jersey Institute of Technology/Rutgers University-Newark 2003. She conducted research investigating the ultrafast photophysics and nonlinear optical properties of Silicon nanostructured materials and single-walled carbon nanotubes.

Anthony M. Johnson has been the Director of the Center for Advanced Studies in Photonics Research and Professor of Physics and Computer Science & Electrical Engineering at the University of Maryland Baltimore County since 2003. He received a BS in Physics (1975) from Polytechnic Institute of New York and a PhD in Physics (1981) from City College of the City University of New York. His current research interests include the ultrafast photophysics and nonlinear optical properties of bulk, nanostructured, and quantum well semiconductor structures, ultrashort pulse propagation in fibres and high-speed light wave systems.

Ronghui Ma currently holds a position of Associate Professor of Mechanical Engineering, University of Maryland Baltimore County. She earned her BS degree from Zhejiang University, 1991, MS degree from Southeast University, 1994 and PhD degree from State University of New York Stony Brook University, 2003, all in Mechanical Engineering. Her research interest is in

computational studies of transport of heat, mass and momentum, phase change, chemical reactions, colloidal fluid flow, etc., using various computational methods such as finite volume/finite element, meshless method, particle tracking and molecular dynamic simulation.

Liang Zhu is an Associate Professor at the Department of Mechanical Engineering in the University of Maryland Baltimore County. She received her BS from the University of Science and Technology of China, Hefei, China, in 1988 and her PhD from the City University of New York, New York, in 1995, all in Engineering. Her research is focused on fundamental heat and mass transfer mechanisms in biological systems and temperature distribution in tissue during hypothermia or hyperthermia treatments in clinical applications.

1   Introduction

In the past decades, growing evidence has suggested the promise of hyperthermia for killing cancer cells. Hyperthermia is preferred for patients diagnosed with previously inoperable or surgically complex tumours, or for patients looking for an alternative to costly and risky surgeries. Tumour temperatures higher than 43°C maintained at sufficient heating duration may produce heat-induced cytotoxic responses and/or increase the cytotoxic effects of radiation and drugs.

Traditional hyperthermia methods include radio frequency (RF), microwave, laser and ultrasound. Clinical evidence (Wong et al., 2009) suggests that RF ablation has high success rates in patients with colorectal cancer, with only a few un-resectable hepatic metastases (<30 mm dia.); in these patients, the five year survival rates varied from 14% to 55%. A recent study (Zou et al., 2010) using RF for un-resectable pancreatic cancer indicated a marked decrease in pain score and improvements in patients. For prostate cancer treatment, local hyperthermia has been considered minimally invasive due to transurethral or transrectal access to the prostate. The effect of RF ablation was examined in another clinical study (Lanuti et al., 2009) for treating inoperable lung cancer and it has shown 78% and 47% survival rates after two years and four years, respectively. It has been reported that focused ultrasound has achieved more than 66–80% success rate in destroying tumours (Chaussy and Thuroff 2001; Gelet et al., 2001). Another hyperthermia approach uses microwaves to elevate the tumour temperatures in the prostate. The microwaves are emitted from an antenna inserted in the prostatic urethra (Homma and Aso 1993; Sapozink et al., 1993; Larson et al., 1996; Sherar et al., 2004; Zhu et al., 2005). These clinical and animal studies provide strong rationale for using hyperthermia approaches to eradicate cancer cells.

Some of the complications associated with those hyperthermia methods may be due to poorly designed heating protocols. All the above approaches require a wave or current to be passed through the tissue; when this wave or current interacts with the molecules in the tissue, heat is generated. However, microwave or RF current decays as it passes through the tissue, resulting in an energy generation density that decays rapidly from the location where it is initiated. In addition, thermal damage to healthy tissue may occur along the paths of the wave or current.

To overcome the limitations of those traditional methods, in recent years, various studies (Bernardi et al., 2008; Gobin et al., 2008; Melancon et al., 2008) have shown that gold nanoshells or nanorods injected into tumours can serve as strong laser energy absorbers to confine laser energy in tumours. It has been suggested (Reidenbach, 2007) that the Near Infrared (NIR) laser with a wavelength of approximately 800 nm may penetrate into normal tissue with minimal laser absorption before reaching the targeted tumour containing nanoshells or nanorods. Due to the powerful optical absorption by nanorods, the laser energy is concentrated in an area congregated by nanorods, and then the energy absorbed can be transferred to the surrounding tumour tissue by heat conduction. Thermal damage to targeted tumour cells is affected by temperature elevations in the tumours and exposure time (Engin, 1994; Welch and van Gemert, 1995; Dewhirst et al., 2005). Designing an optimal heating protocol to cause irreversible thermal damage to tumours relies on a wide range of heating parameters, as well as determination of the minimal thermal dosage for tumours with specific types, growth stages and their surrounding tissue environment.

The feasibility of using gold nanoshells or nanorods to identify laser power settings for tumour destruction has been tested both in tissue culture or phantoms (Sayed et al., 2006; Bernardi et al., 2008; Gobin et al., 2008; Melancon et al., 2008; Norman et al., 2008; Elliott et al., 2010; Krishnan et al., 2010) and in implanted tumours in animal models (Hirsch et al., 2003; O'Neal et al., 2004; Diagaradjane et al., 2008; Stern et al., 2008; Schwartz et al., 2009; Rylander et al., 2011; Stafford et al., 2011; Manuchehrabadi et al., 2012). Most *in vivo* experiments performed on mice involve injecting approximately 0.1–0.2 ml nanoshell solution (concentration varies from 10^9 to 10^{14} nanostructures per ml solution). Typical laser irradiance at the surface is 2–35 W/cm^2 for the photothermal therapy to be effective (Hirsch et al., 2003; O'Neal et al., 2004; El-Sayed et al., 2006; Qin and Bischof, 2010). Laser spot size should affect primarily the tumour region laterally and it varies from 1–5 mm in diameter (Hirsch et al., 2003; Elliott et al., 2007). Heating duration can be shorter than three minutes or longer than 15 minutes (Hirsch et al., 2003; O'Neal et al., 2004; Melancon et al., 2008; Manuchehrabadi et al., 2012). Successful treatments are illustrated by the shrinkage of the tumour following the laser therapy, as well as observed tumour cell death in tissue culture. Some experiments also involve measuring temperatures at various tumour locations (Hirsch et al., 2003; Diagaradjane et al., 2008; Stafford et al., 2011). The temperature elevations and tumour shrinkage are also dependent on the concentration of the nanoshell solutions (Stern et al., 2008; Manuchehrabadi et al., 2012). Recently, our group has demonstrated that using only 0.1 ml of a highly concentrated gold nanorod solution can lead to tumour temperature higher than 48°C when the laser irradiance is 1.6 W/cm^2 (Manuchehrabadi et al., 2012). The laser irradiance used in that study is close to the lower limit of that reported in the previous studies. Based on the measured temperature mapping of two tumour paths, the *in vivo* experimental studies have suggested feasibility of using a 250 Optical Density (OD) gold nanorod solution to induce sufficient temperature elevations in the tumour. Specifically, the tumour temperatures can reach at least 48°C under a laser irradiance of 1.6 W/cm^2 and a laser spot size of 7 mm in diameter if the tumour diameter is smaller than 12 mm. Based on the measured temperature elevations and heating duration, thermal damage to the tumour is most likely to have occurred when using the 250 OD nanorod solutions. However, it is still unclear whether irreversible thermal damage was truly induced, especially in the tumour periphery where the lowest temperatures exist, and whether tumour shrinkage can be ensured after the laser treatment.

Since the ultimate thermal damage depends on temperature elevation history and heating duration, it is important to evaluate simultaneously both temperature elevations and treatment efficacy (histological analyses and tumour shrinkages). The Arrhenius integral (Moritz and Henriques, 1947) can be used to quantitatively assess thermal damage based on measured or simulated temperature history at various tissue locations. Implementing the integral requires knowing the activation energy and the frequency factor associated with the tissue cells. Their values are typically obtained via performing quantitative experimental measurements of cell death percentages when cells are subject to various temperature levels and heating durations. The major challenge is that the magnitudes of the coefficients are cell dependent. Applying one successful treatment protocol (thermal dosage) for one tumour to another may not result in the same level of thermal damage. This is largely due to the fact that heat tolerance varies from one kind of tumours to another, and it may also depend on tumour's growth stages. One previous experimental study of thermal tolerance of various carcinoma cells has demonstrated that human prostatic carcinoma cell lines are much easier to be damaged than carcinoma cell lines of other human origin such as colon, breast, lung and brain, under the same mild hyperthermia dosage (Ryu et al., 1996).

Lethal thermal dosage can also be estimated by the EM_{43}, an alternative parameter derived from the Arrhenius integral varying significantly from one study to another (Diederich, 2005). The EM_{43}, called thermal isoeffective dose, converts the temperature levels and heating duration into an equivalent number of minutes at 43°C to induce irreversible thermal damage to a specific tumour cell type (Sapareto and Dewey, 1984). It can be used to compare thermal dosages of different treatment protocols. A summary by Dewhirst et al. (2003) shows a wide range of EM_{43} values for various tissue types including bone marrow, brain, skin, fat, liver, muscle, etc. It is understandable to have a longer EM_{43} leading to thermal shrinkage of skin and ligament than other soft tissues (Hayashi and Markel, 2001; Diederich, 2005). For the same type of tissue such as liver or muscle, the required EM_{43} for thermal damage varies greatly from one experiment to another (Dewhirst et al., 2003). The EM_{43} can vary from 85 minutes to 540 minutes (Dewhirst et al., 2003; Diederich, 2005) for tumours. Those previous studies have demonstrated complicated biological and chemical factors that may contribute to the wide range of the threshold thermal dosage. It strongly suggests that experimental studies are necessary to evaluate thermal damage to tumours to extract either the coefficients used in the Arrhenius integral or the EM_{43} value, to assess whether a future treatment protocol is likely to induce adequate thermal damage to targeted tumour types.

Another important factor is the temperature range used in hyperthermia treatment. Previous experimental studies using laser photothermal therapy achieve much higher temperature elevations (>50°C) than the traditional mild hyperthermia (43–46°C), where a heating duration of hours is required to result in thermal damage to tissue. One concern raised in the traditional mild hyperthermia is possible thermal tolerance induced by the relatively low tumour temperatures and this is likely to occur when multiple heating sessions are administrated (Bhowmick et al., 2000). In addition, physiological responses of tumours to mild hyperthermia, such as increases in tumour blood flow and oxygenation, heat shock protein releases, etc, can greatly affect the ultimate treatment outcome (Song et al., 2005; Rylander et al., 2011). It has been suggested that administration of a local single dose of thermal therapy utilising temperature > 50°C for short time duration of minutes would address the problems (Bhowmick et al., 2000). It has been shown that thermal damage processes depend on the range of the achieved

temperature elevations in tumour cells (Bhowmick et al., 2000). The large variations of laser irradiance incident on tumour surfaces in previous studies also make it difficult to assess thermal damage to targeted tumour tissue. Therefore, experimental studies to evaluating thermal damage in the same type of tumours at different temperature ranges are essential to provide meaningful treatment protocol based on thermal damage models. Understanding thermal damage to human prostatic cancer cells induced by laser photothermal therapy will fill up the unknown threshold thermal dosage in the high temperature range. Evaluation of a treatment protocol using laser photothermal therapy in an animal model is the first step leading to future optimal designs in clinical settings.

Tumour shrinkage after hyperthermia treatment can be considered as an indication of thermal damage. It is also important to couple experimentally measured temperature elevation history with histological analyses of cell death. Generally, there are several histological markers of non-ablative thermal damage. The type of damage process is recognisable only based on pathological evaluations of laser irradiated tissue. These histological markers reveal whether the temperature elevation and duration of laser irradiance result in recoverable damage or lethal thermal effects. Recoverable damages, such as intracellular edema, thermal inactivation of specific enzymes, as well as cellular membrane rupture, represent situations when cells may tolerate and survive the modest temperature elevations for specific periods of time after the treatment (Kumar et al., 2005). On the other hand, lethal thermal markers are cell death and necrosis. This occurs when the repair mechanisms or their mediators (DNA and RNA enzymes) are thermally disabled (Ghadially and Skinnider, 1976). High temperature thermal damage process may result in denaturalisation of protein structures and conformational changes in energy producing enzymes. One lethal thermal marker visible to naked eyes is coagulation, whitening of the tissue that is associated with increased opacity. Therefore, observation of various markers can be used to evaluate severity and uniformity of thermal damage to entire tumours.

The objective of this study is to measure tumour shrinkage and to perform histologic analyses after laser irradiation to evaluate whether an administrated laser photothermal treatment protocol induces adequate thermal damage to tumours. Histological analyses of the tumours after laser irradiation will be used to evaluate whether irreversible thermal damage occurs in the entire tumour region. Since the heating protocol used in this study is the same as that used in a previous *in vivo* experiment, coupling the histological analyses and tumour shrinkage results with the measured temperature distribution can help identify future optimal treatment protocols in laser photothermal therapy using minimal laser power.

2 Methods and materials

2.1 Animal and tumour models

Twelve BALB/c Nu/Nu male mice (National Cancer Center, 3–6 months old, mean ± SD: 23.8 ± 4.5 g) bearing PC3 xenograft tumours have been used in the study. Prostate cancer PC3 cells grew in a physiological bicarbonate buffering solution (RPMI 1640) and were harvested with trypsin digestion. A total of 10^7 PC3 cells were subcutaneously injected via a 26-gauge needle to the right and left flanks of individual nude mice. Flank

xenografts were observed within 2–3 weeks after the implantation and several positions were measured via a calliper. Once one of the inoculated tumours reached a desired size (at least 10 mm in diameter), it would be subject to laser irradiance, which will be described later in the section. The mouse was anesthetised via Na pentobarbital injections (40 mg/kg, i.p.). During the entire experiment, its body temperature was maintained using a water-jacketed heating pad, and was monitored via a thermocouple inserted in the rectum for the entire experiment. Five mice were used for the tumour shrinkage study and the other seven were for histological analyses.

2.2 Nanorod injection

Gold nanorod solutions (NanPartz™, CO) with a concentration of 250 OD (2.1×10^{14} NPS/ml) were tested in this study. The gold nanorods (GNRs) have an aspect ratio of 4.5 (longitudinal length: 45 nm and transversal diameter: 10 nm). Longitudinal resonance spans at 808 nm while their transverse resonance occurs at about 520 nm. The gold nanorod solution was loaded on a syringe pump with multiple syringe holders (KD Scientific S230, Holliston, MA). After anesthesia, a 26-gauge Hamilton needle (Fischer Scientific, Springfield, NJ) was used for a unilateral injection of 0.1 ml of gold nanorod solutions into the centre of one of the two tumours at an infusion rate of 5 μl/min. The contra-lateral tumour served as the control with neither nanorod injection nor laser irradiation.

2.3 Laser irradiation

The surface of the tumour with the nanorod injection was then irradiated by a Ti:Sapphire laser operating at a wavelength of 800 nm (Spectra Physics, Irvine, CA). The laser irradiance at the tumour surface was fixed at 1.6 W/cm^2 with an average power of 0.6 W and a laser spot of 7 mm in diameter for 15 minutes. Note that the heating protocol in this study is the same as that in a previous work (Manuchehrabadi et al., 2012). After the heating treatment, the mouse was either returned to the animal facility for further tumour shrinkage studies or euthanatised for histological analyses.

2.4 Tumour shrinkage studies

Five mice were used for the tumour shrinkage study. After the heating experiment, the mouse was returned to the animal facility and monitored until it awakened from anaesthesia. The animal facility technician in the Biology Department at UMBC ensured that it was ambulatory and could drink water for five days post-treatment. The mouse was also fed with ibuprofen (200 μg/ml for a dose of 40 mg/kg) in the drinking water for five days post-treatment.

The tumour shrinkage on the irradiated tumour site was compared to the contra-lateral tumour growth to evaluate the treatment efficacy. Within 25 days after the laser treatment, tumour sizes on both flanks (with or without laser irradiation) were carefully monitored and measured. Tumours dimensions were determined via a calliper. For the treated tumour group and control tumour group, the greatest longitudinal diameter (length = L) and the greatest transverse diameter (width = W) were measured. Previous studies (Euhus et al., 1986; Tomayko and Reynolds, 1989) suggested a modified ellipsoidal formula for tumour measurement in nude mice as follows:

$$Tumour\ volume = 1/2\,(L \times W^2) \tag{1}$$

This formula has been shown to provide an accurate estimation of implanted tumour volumes, based on comparisons to that measured by three-dimensional microCT scans and PET imaging technology (Jensen et al., 2008). Both tumours were measured six times during the 25 days after the laser treatment. The mice were eventually euthanised after the tumour shrinkage study via Na pentobarbital overdose (160 mg/kg, i.p.).

2.5   Histological analyses

Seven BALB/c Nu/Nu male mice have been used for histological analysis. After the laser irradiation, the mouse was euthanised via Na pentobarbital overdose (160 mg/kg, i.p.). Then the tumours were resected surgically. The tumours were cut into several small pieces and fixed in a 10% neutral buffered formalin solution for 48 hours at room temperature, dehydrated through an ascending ethanol gradient and embedded in paraffin. Five micron sections were placed on charged glass slides and after deparaffinisation and rehydration, tissues were stained with haematoxylin and eosin. Histological analyses of tumours were performed using light microscopy for observation of cell damage.

2.6   Estimation of EM_{43}

The concept of EM_{43} was introduced by Sapareto and Dewey (1984) to provide a unique parameter to describe the thermal dosage for tissue destruction. Unlike the Arrhenius integral that requires knowing the values of the activation energy and frequency factor of that tissue, EM_{43} is used to quickly evaluate whether a planned treatment protocol will result in adequate thermal damage to a tumour type at certain growth stage, based on previous experimental studies of a time duration (minutes) of inducing lethal damage when the temperature of the same tumour type is elevated quickly to 43°C and maintained at 43°C. It is understandable that the EM_{43} may vary from one tumour to another. The EM_{43} can be calculated by the following equation:

$$EM_{43}\ for\ location\ i = \sum_{j=1}^{n} \Delta t_j R_j^{\,43-T_{i,j}}, \quad total\ heating\ duration = \sum_{j=1}^{n} \Delta t_j \qquad (2)$$

In this equation, the measured temperature elevation history at location i is approximately represented by dividing the total heating duration into individual time segments Δt_j, when the temperature at location i is maintained as a constant. R is called the R-value representing a modification to calculate the equivalent minutes at 43°C from the actual heating duration, Δt_j. It has been demonstrated that the R-value also depends on the temperature range. In this study, we adopt the R-values from a previous study (Dewhirst et al., 2003):

$$R = \begin{cases} 0.25 & 37°C \le T \le 43°C \\ 0.50 & 43°C < T < 48°C \\ 0.72 & 48°C \le T \end{cases} \qquad (3)$$

When the tissue temperature is higher than 43°C, the equivalent minutes at 43°C is longer than the actual heating time. For example, if the temperature is maintained at 45°C

for five minutes (Δt_j), based on equation (2), the equivalent minutes for this time segment will be longer than five minutes with an *R*-value of 0.5. It is calculated by

$$\Delta t_j R^{43-T_{i,j}} = 5\min{}^* R^{43-45} = 5\min{}^* 0.5^{-2} = 20\min \tag{4}$$

Equation (4) suggests that the equivalent minutes at 43°C is approximately 20 minutes when the temperature is 45°C, four times of the actual duration of five minutes at 45°C. On the other hand, when the tissue temperature is maintained at 42°C for ten minutes, based on equation (2), the equivalent minutes at 43°C is calculated as:

$$10\min{}^* 0.25^{43-42} = 2.5\min \tag{5}$$

In another word, the equivalent minutes at 43°C will be shorter than the actual heating time when the tissue temperature is lower than 43°C. The EM_{43} can also be written in an integral form as:

$$EM_{43} \; for \, location \;\; i = \int_0^t R^{43-T_i(t)} dt \tag{6}$$

where $T_i(t)$ describes how the temperature at location *i* changes with time *t*.

3   Results

3.1   *Tumour shrinkage studies*

Figure 1 shows digital photographs of tumours of a mouse before the laser treatment (the left panel) and on the 25th day following the treatment (the right panel). After the laser experiment, one observes that the tumour with the treatment almost disappears completely after 25 days. All scars fall off within the 25 days. In contrast, the control tumour (circled by the solid lines in Figure 1) continues to grow and a considerable volume increase is evident in the image.

Figure 1   Images of a mouse before (left image) and after the laser photothermal therapy (right image)

| Before Laser treatment | After 25 days from treatment |
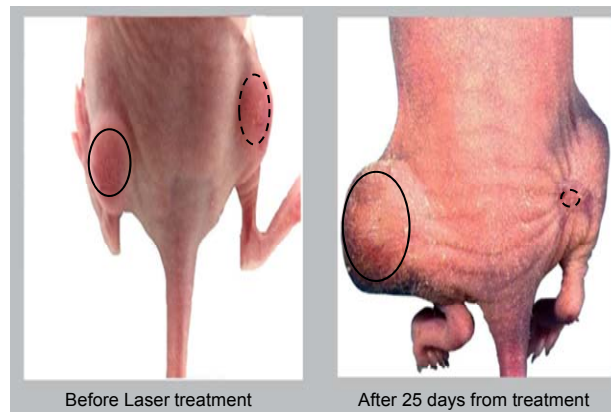
Notes: The solid circle shows the control tumour with neither nanorod injections nor laser irradiation and the dash lined circle shows the laser irradiated tumour.

Table 1 provides the measured tumour geometry and the calculated tumour volume and its standard deviation. Tumour volume changes during the 25 days after the laser treatment are given in Figure 2. This figure shows the initial average tumour size as 691 ± 62 mm^3 (mean $\pm$ SD). Three days later, its average volume decreases to 268 mm^3. Afterwards the tumours continuously shrink. On the 25th day following the treatment, their average volumes are approximately 44.7 mm^3, which is only 7% of its initial value. Statistical analyses of the average tumour volume after specific days post-treatment is compared to the initial average volume are performed via the student *t*-test. As shown in Figure 2, the difference between individual groups (3, 6, 11, 18, 19 and 25 days post-treatment) and the initial group before the laser treatment on day 0 are statistically significant with a *p*-value less than 0.05.

Figure 2   Average tumour volumes before (day 0) and after the laser treatment (3, 6, 11, 18 and 25 days post treatment) in the irradiated tumour group ($n = 5$)
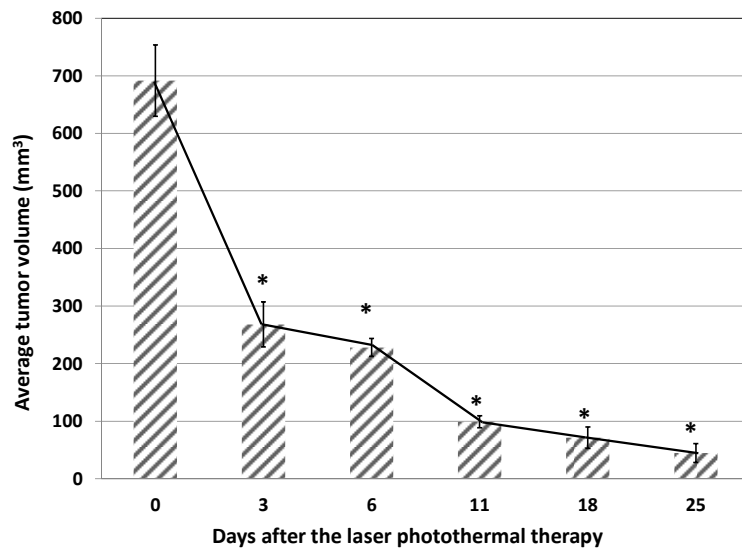
Notes: * represents a statistically significant difference ($p < 0.05$) between the tumour volume after specific days post-treatment and the initial tumour volume (day 0).

Table 1   Measured size parameters of the initial tumour volumes

	The tumours in the heating group					The tumours in the control group				
	1	2	3	4	5	1	2	3	4	5
Longitudinal diameter L (mm)	12.75	13.87	13.00	11.50	11.20	11.73	10.59	7.80	6.40	5.28
Transverse diameter W (mm)	9.98	10.53	10.30	11.20	10.90	7.21	7.32	7.30	5.10	6.21
Volume (mm^3)	635	769	690	721	666	305	284	208	83	102
Mean volume (mm^3)			691					193		
SD (mm^3)			62					115		

The initial average tumour volume in the untreated group is 193 ± 115 mm^3 (Table 1). The smaller initial volume is due to our tendency to select the bigger tumour from both flanks for the heating experiment. The large standard deviation in this group may be attributed to the fact that those tumours in the control group are not developing at the same rate. In contrast to the irradiated tumours, the tumour volumes in the untreated

group increase drastically within the 25 days, as shown in Figure 3. Initially, the tumour growth is slow; however, the growth is accelerated in later days. Figure 3 shows that the average tumour volume in the control group on the 25th day has reached 560 ± 83 mm^3, which is 2.5 times of the initial size.

Figure 3   Average tumour volumes before (day 0) and after (3, 6, 11, 18 and 25 days after the date of the laser photothermal therapy) in the untreated group ($n = 5$)
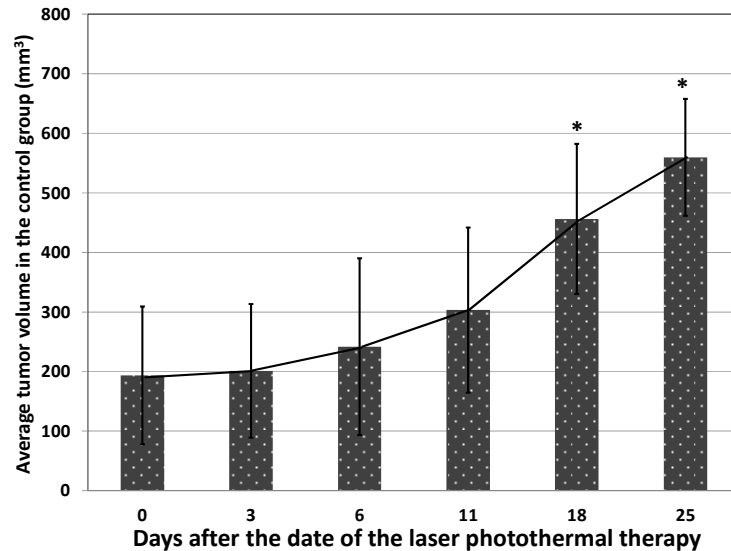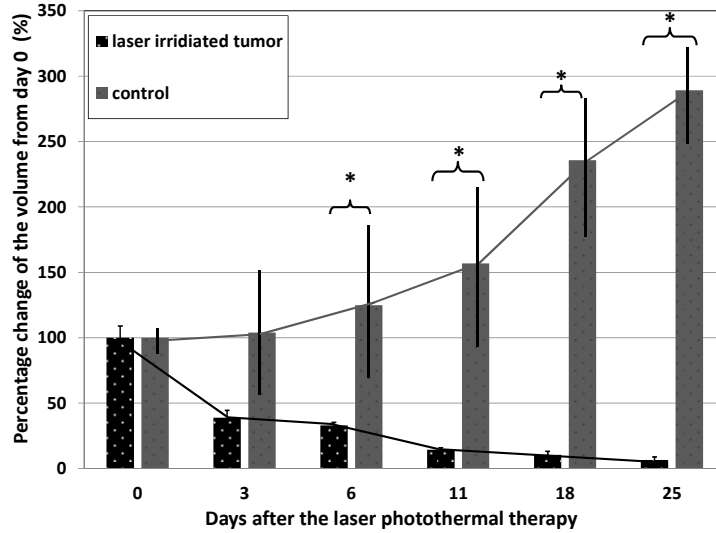

Notes: * represents a statistically significant difference ($p < 0.05$) between the tumour volume after specific days and the initial tumour volume on day 0.

The comparison between the untreated and laser irradiated tumour groups is illustrated in Figure 4, in terms of the percentage volume change. Overall, tumour shrinkage in the irradiated group is evident and its size is decreased by half within three days, and after 25 days it almost disappears from the site. On the other hand, the tumour size of the untreated group continues to grow and its size doubles after 18 days. We also compare the percentage volume changes of the untreated group to that of the irradiated group after the same number of days post-treatment to determine whether they are statistically different with a *p*-value less than 0.05 (6, 11, 18 and 25 days post-treatment), using the student *t*-test.

3.2   *Histological analyses*

Histological analyses of the tumours after laser heating are performed using light microscopy. Examination of a typical haematoxylin and eosin stained tumour section is shown in Figure 5, where the cell nuclei are stained purple while the cytoplasm appears pink. Broad areas of largely necrotic tissue are apparent towards the tumour centre, whereas more peripheral regions are characterised by cells with abnormal-appearing chromatin and interspersed apoptotic nuclei. A zone of mixed apoptotic and necrotic events was apparent at the junction between these zones (Figure 5). An acute inflammatory infiltrate was also present, as evidenced by the presence of polymorphonuclear granulocytes. The entire tumour was essentially devoid of mitotic figures.

Figure 4 Percentages of tumour volume changes from its initial volume on day 0 ($n = 5$)

Notes: *demonstrates a statistically significant difference between the percentage change of the untreated group and that of the irradiated group after specific days post-treatment with a p-value smaller than 0.05.

Figure 5 Histologic images of a tumour tissue section
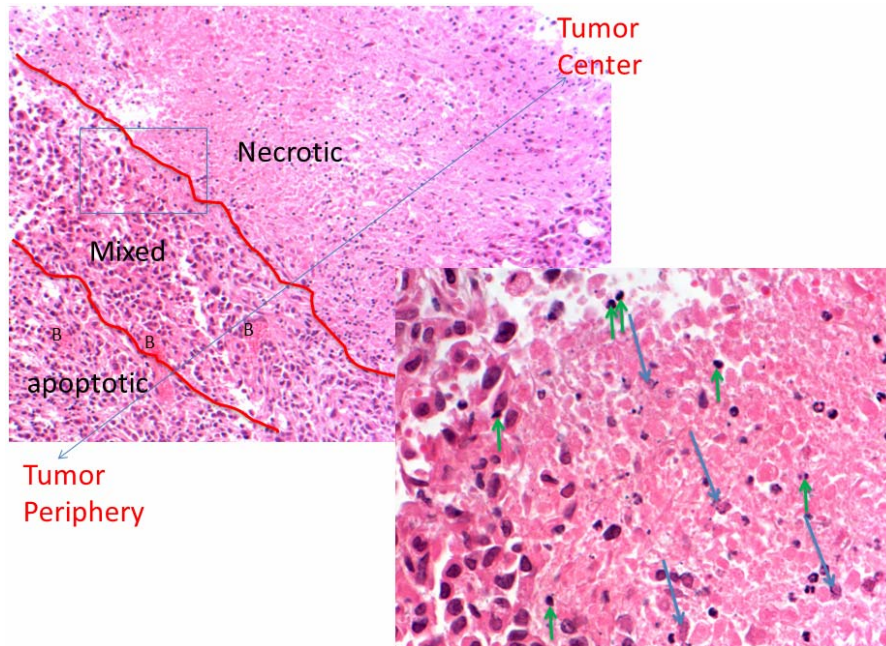
Notes: The image on the right side is the enlarged rectangular region on the left panel. Thermally damaged tissue is characterised by zones that are largely necrotic and areas of mixed apoptosis/necrosis. Short green arrows: apoptotic nuclei, long blue arrows: necrotic cells, B: blood vessels.

3.3 EM_{43} calculations

Table 2 gives the steady state temperature elevations recorded in the previous experiments (Manuchehrabadi et al., 2012). In the previous study, temperature mapping along tissue paths in a plane perpendicular to the laser direction are recorded via pulling thermocouples from one side of the tumour periphery, into the deep tumour region, and out from the other tumour periphery. Considering that the laser has to penetrate from the top tumour surface to the deep region along the laser direction, two paths are selected so that one path (Path I) is located on a plane perpendicular to the laser direction and the plane is located approximately half of the tumour diameter beneath the tumour top surface, while temperatures along the other tumour path (Path II) is on a plane with a vertical distance of approximately three fourth of the tumour diameter. It is expected that the temperature elevations along Path II would be smaller than that along Path I.

Table 2   Measured temperatures at various tumour locations and the calculated EM_{43} values

r (mm)	–6	–4	–2	0	2	4	6
Temperature along Path I (°C)	55.3	58.3	58.9	61.0	57.9	54.0	51.4
EM_{43} along Path I (min)	616	1632	1984	3994	1433	404	174
Temperature along Path II (°C)	54.2	54.6	55.0	57.2	54.1	50.1	48.0
EM_{43} along Path II (min)	431	491	559	1141	417	115	67

Notes: The maximal temperature along each path is represented by $r = 0$ mm, while other r values give the distance from the maximal temperature location.

Source: Manuchehrabadi et al. (2012)

A steady state temperature field in the tumour was typically established within five minutes after the laser was turned on, and the heating was continued for another ten minutes (Manuchehrabadi et al., 2012). Two thermocouples were inserted and the steady state temperatures along the tissue paths were recorded for ten minutes after the steady state was established (Manuchehrabadi et al., 2012). In this study, we assume that the temperature increased linearly from its baseline of 37°C to its steady state temperature T_{ss} within the first five minutes. Given in Table 2, the maximal tumour temperature (61°C) occurs at the tumour centre along Path I, while the minimal temperature (48°C) occurs at the tumour peripheral along Path II (Manuchehrabadi et al., 2012). The following equations show how the EM_{43} is calculated using equation (6) with the R-values given in equation (3).

$$EM_{43,max} = \int_0^5 R^{43-[37+(61-37)t/5]}dt + 10*0.72^{43-61} = 296 + 3698 = 3994 \min$$

$$EM_{43,min} = \int_0^5 R^{43-[37+(48-37)t/5]}dt + 10*0.72^{43-48} = 18.7 + 48.4 = 67 \min$$

(7)

where the R-value may vary since the integral covers a large temperature range. The first term in equation (7) gives the equivalent minutes at 43°C from the first five minutes, while the second term shows the equivalent minutes from ten minutes after the steady state. The primary contribution to the EM_{43} is from the steady state (the 2nd term in equation (7)) when the tumour temperatures are higher. Note the wide range of thermal dosages (EM_{43}) within the tumour in Table 2. Among the 14 tumour locations, 11 of

them (79%) have an EM_{43} longer than 400 minutes. Except the one location at the tumour periphery, 93% of the tumour locations (13/14 = 0.93) have an EM_{43} longer than 110 minutes. Nevertheless, the lower thermal dosage occurring at the tumour periphery is consistent with the less severe thermal damage observed in the histological analyses.

4 Discussions

Laser photothermal therapy has the potential for treating local prostatic tumours. For prostatic cancer treatment, regional hyperthermia has been considered minimally invasive due to transurethral or transrectal access to the prostate. Temperature elevations in tumours can be induced via laser energy emitted from a laser catheter inserted in the prostatic urethra. Utilising near-infrared laser at a wavelength of 800 nm provides an advantage to minimise laser energy absorption by the prostatic tissue near the prostatic urethra, therefore, maximising heat absorption by the prostatic tumour with nanorods. This goal can be achieved by carefully designing heating protocols via theoretical simulations before the actual laser treatment. Therefore, understanding the minimal thermal dosage (EM_{43}) to a specific prostatic tumour type is important to design optimal heating protocols for prostatic cancer patients.

Laser photothermal therapy has shown potential of confining almost 100% of the laser energy to targeted tumours if sufficient nanorods are delivered to the tumour. Using direct intratumoural injections of gold nanorod solution to tumours has the advantage over systemic intravenous delivery, since it can be effective to deposit nanorods to targeted tumours even if the tumours are poorly and/or non-uniformly perfused. Using a highly concentrated gold nanorod solution, previous experiments have shown feasibility of elevating the tumour temperature to up to 61°C at the tumour centre and at least 48°C at the tumour periphery. Due to the lack of temperature recordings before the steady state was established (Manuchehrabadi et al., 2012), the EM_{43} shown in Table 2 is calculated based on a linear rising from 37°C to T_{ss} for the initial five minutes. This is certainly a limitation of this study. However, as shown in Equation 7, the contribution to the EM_{43} from the period before the steady state was established is small when the temperature elevations are much higher than 43°C. Future studies are needed to have a precise temperature elevation history during heating to have a more accurate estimate of the EM_{43}.

The EM_{43} of tumours obtained from previous studies vary from 85 minutes to 540 minutes (Engin, 1994; Dewhirst et al., 2003; Diederich, 2005). It is evident that the temperature elevations are based on the sizes of the tumour and the laser spot. The laser spot size in our study is fixed as 7 mm in diameter. Table 2 illustrates that a minimal temperature of 50°C can be established at the tumour periphery if the tumour diameter is less than 8 mm in diameter, however, the peripheral temperature is only 48°C if the tumour is approximately 12 mm in diameter. For a spherical tumour with a volume of 904 mm^3 (12 mm in diameter), the minimal EM_{43} is 67 minutes. However, 93% of the tumour region will have an EM_{43} longer than 110 minutes, and 79% will have an EM_{43} longer than 400 minutes. Based on comparing the calculated EM_{43} values to that in previous studies, it is highly likely that the proposed heating protocol should have caused lethal thermal damage to the majority region of the tumours.

The major finding of this study is that the observed tumour shrinkage supports the hypothesis that the heating protocol used in a previous experiments causes thermal

damage to the tumours. Despite the variation of the initial tumour volumes (635–769 mm^3) before the laser treatment, measured tumour volumes following the laser treatment confirm a significant decrease in the tumour sizes, which is believed to be induced by the laser photothermal therapy using gold nanorods. Our results are consistent with that by other groups. A previous study (O'Neal et al., 2004) utilising a laser irradiance of 4 W/cm^2 for three minutes has shown complete resorptions of the studied tumours (subcutaneous murine colon carcinoma) within only ten days following the heating experiment. In contrast, all sham and control group mice have shown continuous growths of the tumours so that all the mice in those two groups have to be euthanised by day 19. Injecting a high dose of gold nanoshell solution (3x10^9 GNS/ml) to implanted prostatic tumours (PC3) and irradiating the tumour surface with an NIR laser (4 W/cm^2) for three minutes have resulted in complete tumour involution within 21 days of the tumour shrinkage study (Stern et al., 2008). Another study (von Maltzahn et al., 2009) proposes a computationally designed irradiation regimen (810 nm, 2 W/cm^2, five minutes) using gold nanorods for maximising laser energy absorption in tumours. In that study the relative tumour volume changes in four groups of tumours (nanorod + laser, nanorod alone, laser alone and saline injection alone) are measured and recorded for 20 days. Only the tumour group with laser treatment enhanced by nanorod injections shows continuous volume shrinkage. In the other three groups tumour volumes increase up to 5 folds from their original values. It must be noted that all the previous studies have utilised a much larger laser irradiance (2–4 W/cm^2 vs. 1.6 W/cm^2) incident on the tumour surface, although the gold nanorod solution in our study is more concentrated than that of the previous studies.

Histological analyses of tumour cell death are an important part of this study to confirm treatment efficacy using the heating protocol. The observed non-uniform severity of thermal damage in the tumour region are consistent with the non-uniform temperature elevations demonstrated in our previous experimental study (Manuchehrabadi et al., 2012), where the highest temperature elevation occurs in the tumour's central region on which the laser spot is focused. It has been shown that more than 61°C has been reached at the tumour centre. Therefore, it is expected to see that hyperthermia-generated damage of malignant prostate tumour cells is confirmed by the pathological examination of tumour tissue. Although tumour cells may have good thermal tolerance to temperature elevations, the tumour cells heated to a temperature of 61°C in our study suffer irreversible damage leading to of necrosis. On the other hand, thermal damage to the tumour periphery may be at a stage between recoverable and irreversible thermal damage due to a relatively lower temperature elevation to 48°C. Histological analyses have demonstrated that more peripherally localised tumour cells show evidence of chromatin damage and a relatively high incidence of apoptosis.

One limitation of this study is the short observation period of 25 days after the heating experiments. This is largely due to our original experimental design of having the treated and untreated tumours on the same mouse. A much longer period such as 60 days for the tumour shrinkage study is preferred since it may demonstrate that the treated tumour would have grown back. Unfortunately, in our study, the untreated tumour continuously grows over the 25 days, and the mice are under great stress with big tumours on their bodies, necessitating that the mice have to be euthanised. Another limitation of the study is the use of a tumour model implanted on skin surfaces. It is unclear how accurate those tumour models capture human malignancy in deep seated tumours, and whether the distribution of nanostructures and thermal tolerance by tumours

are affected by the tumour location. Future studies are warranted to test laser photothermal therapy in tumour models mimicking realistic human tumours. In addition, the focus of this study is on the PC3 tumour, one of several human prostatic tumours affecting patients. Although the study has showed the effectiveness of using a heating protocol to induce permanent thermal damage to the PC3 tumours, it may not indicate the effectiveness of the heating protocol to other forms of prostatic tumours. It is well known that different kinds of tumours may have different thermal tolerances to heating. Therefore, the EM_{43} may not be the same from one tumour to another. Future experimental studies are needed to determine tumour-type specific thermal dosages.

In summary, in vivo experiments have been performed to induce temperature elevations in implanted prostatic tumours in mice using laser photothermal therapy. 0.1 ml gold nanorod solution is injected to the tumour to maximise NIR laser energy absorption in the tumours. Following the same heating protocols as in our previous experiments, the tumour shrinkage studies and histological analyses of tumour cell death are conducted to confirm treatment efficacy using laser photothermal therapy. It has been shown that the 15 minutes laser heating on tumour tissue containing gold nanorods is effective to cause irreversible thermal damage to tumour, with low laser irradiance on the tumour surface (1.6 W/cm^2). By average, the tumours shrink to less than 7% of its original volume within 25 days after the heating treatment. On the contrast, the tumours without heating continue to grow and double their sizes within 18 days. The histological analyses also demonstrate tumour necrosis events surrounding the tumour centre. However, the extent of thermal damage to the tumour is not uniform throughout. In conclusion, the results in this study have indicated effectiveness of the heating protocols of a previous study for killing tumour cells in implanted PC3 tumours and it is consistent with thermal damage assessment of EM_{43} estimated by possible temperature elevation history during the treatment. It has shown that more than 79% of the tumour locations have an EM_{43} longer than 400 minutes, while 93% of them have an EM_{43} longer than 110 minutes. The lowest EM_{43} value occurs at the tumour periphery.

Acknowledgements

References

Bernardi, R.J., Lowery, A.R., Thompson, P.A., Blaney, S.M. and West, J.L. (2008) 'Immunonanoshells for targeted photothermal ablation in medulloblastoma and glioma: an in vitro evaluation using human cell lines', *Journal of Neuro-Oncology*, Vol. 86, No. 2, pp.165–172.

Bhowmick, S., Swanlund, D.J. and Bischof, J.C. (2000) 'Supraphysiological thermal injury in dunning AT-1 prostate tumor cells', *ASME Journal of Biomechanical Engineering*, Vol. 122, No. 1, pp.51–59.

Chaussy, C. and Thuroff, S. (2001) 'Results and side effects of high-intensity focused ultrasound in localized prostate cancer', *Journal of Endourology*, Vol. 15, No. 4, pp.437–440.

Dewhirst, M.W., Vuhaskovic, Z., Jones, E. and Thrall, D. (2005) 'Re-setting the biologic rationale for thermal therapy', *International Journal of Hyperthermia*, Vol. 21, No. 8, pp.779–790.

Dewhirst, M.W., Viglianti, B.L., Lora-Michiels, M., Hanson, M. and Hoopes, P.J. (2003) 'Basic principles of thermal dosimetry and thermal thresholds for tissue damage from hyperthermia', *International Journal of Hyperthermia*, Vol. 19, No. 3, pp.267–294.

Diagaradjane, P., Shetty, A., Wang, J.C., Elliott, A.M., Schwartz, J., Shentu, S., Park, H.C., Deorukhar, A., Stafford, R.J., Cho, S.H., Tunnel, J.W., Hazle, J.D. and Krishnan, S. (2008) 'Modulation of in vivo tumor radiation response via gold nanoshell-mediated vascular-focused hyperthermia: characterizing an integrated antihypoxic and localized vascular disrupting targeting strategy', *Nano Letters*, Vol. 8, No. 5, pp.1492–1500.

Diederich, C.J. (2005) 'Thermal ablation and high-temperature thermal therapy: overview of technology and clinical implementation', *International Journal of Hyperthermia*, Vol. 21, No. 8, pp.745–753.

Elliott, A.M., Shetty, A.M., Wang, J., Hazle, J.D. and Stafford, R.J. (2010) 'Use of gold nanoshells to constrain and enhance laser thermal therapy of metastatic liver tumours', *International Journal of Hyperthermia*, Vol. 26, No. 5, pp.434–440.

Elliott, A.M., Stafford, R.J., Schwartz, J., Wang, J., Shetty, A.M., Bourgoyne, C., O'Neal, P. and Hazle, J.D. (2007) 'Laser-induced thermal response and characterization of nanoparticles for cancer treatment using magnetic resonance thermal imaging', *Medical Physics*, Vol. 34, No. 7, pp.3102–3108.

El-Sayed, I.H., Huang, X. and El-Sayed, M.A. (2006) 'Selective laser photo-thermal therapy of epithelial carcinoma using anti-EGFR antibody conjugated gold nanoparticles', *Cancer Letter*, Vol. 239, No. 1, pp.129–135.

Engin, K. (1994) 'Biological rationale for hyperthermia in cancer treatment (II)', *Neoplasma*, Vol. 41, No. 5, pp.277–283.

Euhus, D.M., Hudd, C., LaRegina, M.C. and Johnson, F.E. (1986) 'Tumor measurement in the nude mouse', *Journal of Surgical Oncology,* Vol. 31, No. 4, pp.229–234.

Gelet, A., Chapelon, J.Y., Bouvier, R., Rouviere, O., Lyonnet, D. and Dubernard, J.M. (2001) 'Transrectal high intensity focused ultrasound for the treatment of localized prostate cancer: factors influencing the outcome', *European Urology*, Vol. 40, No. 2, pp.124–129.

Ghadially, F.N. and Skinnider, L.F. (1976) '*Chloramphenicol-induced mitochondrial and ultrastructural changes in hemopoietic cells*', *Archives of Pathology and Laboratory Medicine*, Vol. 100, No. 11, pp.601–605.

Gobin, A.M., Moon, J.J. and West, J.L. (2008) 'EphrinAl-targeted nanoshells for photothermal ablation of prostate cancer cells', *International Journal of Nanomedicine*, Vol. 3, No. 3, pp.351–358.

Hayashi, K. and Markel, M.D. (2001) 'Thermal capsulorrhaphy treatment of shoulder instability: basic science', *Clinical Orthopedic Related Research*, Vol. 390, pp.59–72.

Hirsch, L.R., Stafford, R.J., Bankson, J.A., Sershen, S.R., Rivera, B., Price, R.E., Hazlet, J.D., Halas, N.J. and West, J.L. (2003) 'Nanoshell-mediated near-infrared thermal therapy of tumors under magnetic resonance guidance', *Proceedings of the National Academy of Sciences of the United States of America*, Vol. 100, No. 3, pp.13549–13554.

Homma, Y. and Aso, Y. (1993) 'Transurethral microwave thermotherapy for benign prostatic hyperplasia: a 2-year follow-up study', *Journal of Endourology*, Vol. 7, No. 3, pp.261–265.

Jensen, M.M., Jorgensen, T., Binderup, T. and Kjaer, A. (2008) 'Tumor volume in subcutaneous mouse xenografts measured by microCT is more accurate and reproducible than determined by 18F-FDG-microPET or external caliper', *BMC Medical Imaging*, Vol. 8, p.16.

Krishnan, S., Diagaradjane, P. and Cho, S.H. (2010) 'Nanoparticle-mediated thermal therapy: Evolving strategies for prostate cancer therapy', *International Journal of Hyperthermia*, Vol. 26, No. 8, pp.775–789.

Kumar, V., Cotran, R.S. and Robbins, S.L. (2005) *Robbins Basic Pathology*, Elsevier.

Larson, T.R., Bostiwick, D.G. and Corica, A. (1996) 'Temperature-correlated histopathologic changes following microwave thermoablation of obstructive tissue in patients with benign prostatic hyperplasia', *Urology*, Vol. 47, No. 4, pp.463–469.

Lanuti, M., Sharma, A., Digumarthy, S.R., Wright, C.D., Donahue, D.M., Wain, J.C., Mathisen, D.J. and Shepard, A.O. (2009) 'Radiofrequency ablation for treatment of medically inoperable stage I non-small cell lung cancer', *Journal of Thoracic and Cardiovascular Surgery*, Vol. 137, No. 1, pp.160–166.

Manuchehrabadi, N., Attaluri, A., Cai, H., Edziah, R., Lalanne, E., Bieberich, C., Ma, R., Johnson, A.M. and Zhu, L. (2012) 'MicroCT imaging and in vivo temperature elevations in implanted prostatic tumours in laser photothermal therapy using gold nanorods', *ASME Journal of Nanotechnology in Engineering and Medicine*, Vol. 3, No. 2, pp.1–7.

Melancon, M.P., Lu, W., Yang, Z., Zhang, R., Cheng, Z., Elliot, A.M., Stafford, J., Olson, T., Zhang, J.Z. and Li, C. (2008) 'In vitro and in vivo targeting of hollow gold nanoshells directed at epidermal growth factor receptor for photothermal ablation therapy', *Molecular Cancer Therapeutics*, Vol.7, No. 6, pp.1730–1739.

Moritz, A.R. and Henriques, F.C. (1947) 'The relative importance of time and surface temperature in the causation of cutaneous burns', *American Journal of Pathology*, Vol. 23, No. 5, pp.695–720.

Norman, R.S., Stone, J.W., Gole, A., Murphy, C.J. and Sabo-Attwood, T.L. (2008) 'Targeted photothermal analysis of the pathogenic bacteria, pseudomonas aeruginosaa with gold nanorods', *Nano Letters*, Vol. 8, No. 1, pp.302–306.

O'Neal, D.P., Hirsch, L.R., Halas, N.J., Payne, J.D. and West, J.L. (2004) 'Photo-thermal tumor ablation in mice using near infrared-absorbing nanoparticles', *Cancer Letters*, Vol. 209, No. 2, pp.171–176.

Qin, Z. and Bischof, J.C. (2010) 'One dimensional experimental setup to study the heating of nanoparticle laden systems', *Proceedings of Summer Bioengineering Engineering Conference*, 16–19 June, Naples, Florida, USA, pp.81–82.

Reidenbach, H.D. (2007) *Laser Safety, Handbook of Laser and Optics*, Springer.

Rylander, M.N., Stafford, J., Hazle, J., Whitney, J. and Diller, K.R. (2011) 'Heat shock protein expression and temperature distribution in prostate tumours treated with laser irradiation and nanoshells', *International Journal of Hyperthermia*, Vol. 27, No. 8, pp.791–801.

Ryu, S., Brown, S.L., Kim, S.H., Khil, M.S. and Kim, J.H. (1996) 'Preferential radiosensitization of human prostatic carcinoma cells by mild hyperthermia', *International Journal of Radiation Oncology Biology Physics*, Vol. 34, No. 1, pp.133–138.

Sapareto, S.A. and Dewey, W.C. (1984) 'Thermal dose determination in cancer therapy', *International Journal of Radiation Oncology Biology Physics*, Vol. 10, No. 6, pp.787–800.

Sapozink, M.D., Stuart, D.B., Astrahan, M.A., Jozsef, G. and Petrovich, Z. (1993) 'Transurethral hyperthermia for benign prostatic hyperplasia: preliminary clinical results', *Journal of Urology*, Vol. 143, pp.944–950.

Schwartz, J.A., Shetty, A.M., Price, R.E., Stafford, R.J., Wang, J.C., Uthamanthil, R.K., Pham, K., McNicholas, R.J., Coleman, C.L. and Payne, J.D. (2009) 'Feasibility study of particle-assisted laser ablation of brain tumors in orthotopic canine model', *Cancer Research*, Vol. 69, No. 4, pp.1659–1667.

Sherar, M.D., Trachtenberg, J., Davidson, S.R. and Gertner, M.R. (2004) 'Interstitial microwave thermal therapy and its application to the treatment of recurrent prostate cancer', *International Journal of Hyperthermia*, Vol. 20, No. 7, pp.757–768.

Song, C.W., Park, H.J., Lee, C.K. and Griffin, R. (2005) 'Implications of increased tumor blood flow and oxygenation caused by mild temperature hyperthermia in tumor treatment', *International Journal of Hyperthermia*, Vol. 21, No. 8, pp.761–767.

Stafford, R.J., Shetty, A., Elliott, A.M., Schwartz, J.A., Goodrich, G.P. and Hazle, J.D. (2011) 'MR temperature imaging of nanoshell mediated laser ablation', *International Journal of Hyperthermia*, Vol. 27, No. 8, pp.782–790.

Stern, J.M., Stanfield, J., Kabbani, W., Hsieh, J.T. and Cadeddu, J.A. (2008) 'Selective prostate cancer thermal ablation with laser activated gold nanoshells', *Journal of Urology*, Vol. 179, No. 2, pp.748–753.

Tomayko, M.M. and Reynolds, C.P. (1989) 'Determination of subcutaneous tumor size in athymic (Nude) mice', *Cancer Chemotherapy and Pharmacology,* Vol. 24, No. 3, pp.148–154.

von Maltzahn, G., Park, J.H., Agrawal, A. and Bandaru, N.K. (2009) 'Computationally guided photothermal tumor therapy using long-circulating gold nanorod antennas', *Cancer Research*, Vol. 69, No. 9, pp.3892–3900.

Welch, A.J. and van Gemert, M.J. (1995) *Optical-Thermal Response of Laser-Irradiated Tissue*, Plenum Press, New York.

Wong, S.L., Mangu, P.B., Choti, M.A., Crocenzi, T.S., Dodd, G.D., Eng, C., Fong, Y., Giusti, A.F., Lu, D., Marsland, T.A., Michelson, R., poston, G.J., Schrag, D., Seidenfeld, J. and Benson, A.B. (2010) 'American Society of Clinical Oncology 2009 Clinical evidence review on radiofrequency ablation of hepatic metastases from colorectal cancer', *Journal of Clinical Oncology*, Vol. 28, No. 3, pp.493–508.

Zhu, L., Pang, L. and Xu, L.X. (2005) 'Simultaneous measurements of local tissue temperature and blood perfusion rate in the canine prostate during radio frequency thermal therapy', *Biomechanics and Modeling in Mechniobiology*, Vol. 4, No. 1, pp.1–9.

Zou, Y-P., Li, W-M., Zheng, F., Li, F-C., Huang, H., Du, J-D. and Liu, H-R. (2010) 'Intraoperative radiofrequency ablation combined with 125 iodine seed implantation for unresectable pancreatic cancer', *World Journal of Gastroenterology*, Vol. 16, No. 40, pp.5104–5110.